

tems, Foster City, Calif., USA) or an HP G1005A Protein Sequencing System (Hewlett-Packard, Palo Alto, Calif., USA); each fragment was analyzed for 5 cycles.

Carboxymethylation and Peptide Mapping Using Liquid Chromatography/Mass Spectrometry/Mass Spectrometry (LC/MS/MS)

The digested OVM sample was separated electrophoretically as described above, stained with CBB, and the stained bands were cut out. The gel pieces were homogenized in 20 mM Tris-HCl (pH 8.0) containing 0.1% SDS and the proteins were extracted. The extracts were concentrated and purified by acetone precipitation. The acetone precipitates were incubated with 2-mercaptoethanol (92.5 mM) in 72 μ l of 0.5 M Tris-HCl buffer (pH 8.6) containing 8 M guanidine hydrochloride and 5 mM EDTA at room temperature for 2 h. To this solution, 1.5 mg of monoiodoacetic acid was added, and the mixture was incubated at room temperature for 2 h in the dark. The reaction mixture was desalted using a MicroSpin G-25 column (Amersham Bioscience, Uppsala, Sweden) and lyophilized. Reduced and carboxymethylated proteins were digested with trypsin (50 ng/ μ l in 50 mM NH_4HCO_3).

Tandem electrospray mass spectra were recorded using a hybrid quadrupole/time-of-flight spectrometer (Qstar Pulsar i; Applied Biosystems, Foster City, Calif., USA) interfaced to a CapLC (Magic 2002; Michrom BioResources, Auburn, Calif., USA). Samples were dissolved in water and injected into a C18 column (0.2 \times 50 mm, 3 μ m, Magic C18, Michrom BioResources). Peptides were eluted with a 5–36% acetonitrile gradient in 0.1% aqueous formic acid over 60 min at a flow rate of 1 μ l/min after elution with 5% acetonitrile for 10 min. The capillary voltage was set to 2,600 V, and data-dependent MS/MS acquisitions were performed using precursors with charge states of 2 and 3 over a mass range of 400–2,000.

Western Blotting of Digested Fragments with Human Serum IgE

The digested OVM samples were applied to a 10–20% polyacrylamide Tris/Tricine 2D gel, followed by electrical transfer to a nitrocellulose membrane. The membrane was then blocked with 0.5% casein-PBS (pH 7.0) and cut into 4-mm strips. The strips were incubated with diluted human serum (1/4 to 1/5) in 0.2% casein-PBS (pH 7.0) at room temperature for 1 h and then at 4°C for 18 h. After washing with 0.05% Tween 20-PBS, the strips were incubated with rabbit anti-human IgE (Fc) antibodies (Nordic Immunological Laboratories, Tilburg, The Netherlands) at room temperature for 1 h, and then with horseradish peroxidase-conjugated donkey anti-rabbit Ig antibodies (Amersham Biosciences, Little Chalfont, UK) at room temperature for 1 h. Finally, the strips were reacted with Konica ImmunoStain HRP-1000 (Konica, Tokyo, Japan), according to the manufacturer's protocol.

Results

Kinetics of OVM Digestion by Pepsin

OVM was digested in SGF containing various concentrations of pepsin, and the fragments were separated by SDS-PAGE and stained with CBB (fig. 1). The molecular weight of OVM, based on its amino acid sequence, is about 20 kDa, but a broad band representing intact OVM

appeared at about 34–49 kDa in the SDS-PAGE gel because of the presence of five N-linked sugar chains. The pepsin band was detected at 39 kDa, overlapping with the intact OVM band, and lysozyme (14 kDa) contamination was detected in the OVM sample that was used. Intact OVM rapidly disappeared within 0.5 min in SGF (pepsin/OVM = 10 unit/ μ g), and a fragment band was detected at 7 kDa. When the pepsin content in SGF was reduced to 1 and 0.1 unit/ μ g, the digestion rate markedly decreased. Intact OVM was still detected after 30 min when the pepsin/OVM ratio was 0.1 unit/ μ g. The fragment bands were clearer (fig. 2) when a concentrated SGF-digested OVM solution (pepsin/OVM = 1 unit/ μ g, digestion times 5 and 30 min) was used, followed by SDS-PAGE. As shown in figure 2, a strong 23.5- to 28.5-kDa band (FR 1) was detected at 5 min, while 10- (FR 2), 7- (FR 3) and 4.5- to 6-kDa (FR 4) bands were detected after 30 min. FR 1 and FR 2 were both positively stained by PAS, suggesting that the FR 1 and FR 2 fragments have high carbohydrate contents. The time courses for the amounts of intact OVM and the four fractions are plotted in figure 3, where the pepsin/OVM ratio is 1 unit/ μ g. FR 1 rapidly increased but slowly disappeared after 2 min. FR 2 and FR 3 also rapidly reached maximum values at 5 min and then slowly disappeared. On the other hand, FR 4 gradually increased throughout the entire period of the experiment.

Preheating (at 100°C for 5 or 30 min) of the OVM solution (5 mg/ml in water) did not influence the digestion pattern (fig. 1).

Table 1. N-Terminal sequences of pepsin fragments

Digestion period	Fraction	Fragment Residues	Sequence	Ratio % ^a	
5 min	FR 1	1-1	50-54	FGTNI	73.1
		1-2	51-55	GTNIS	11.6
		1-3	1-5	AEVDC	6.9
5 min	FR 2	2-1	1-5	AEVDC	68.8
		2-2	134-138	VSVDC	28.2
5 min	FR 3	3-1	1-5	AEVDC	48.4
		3-2	134-138	VSVDC	24.3
		3-3	104-108	NECLL	9.6
		3-4	85-89	VLCNR	6.5
30 min	FR 4	4-1	134-138	VSVDC	30.6
		4-2	104-108	NECLL	24.0
		4-3	19-23	VLVCN	20.6

^a Molar ratios of the fragments to the total amount in each fraction.

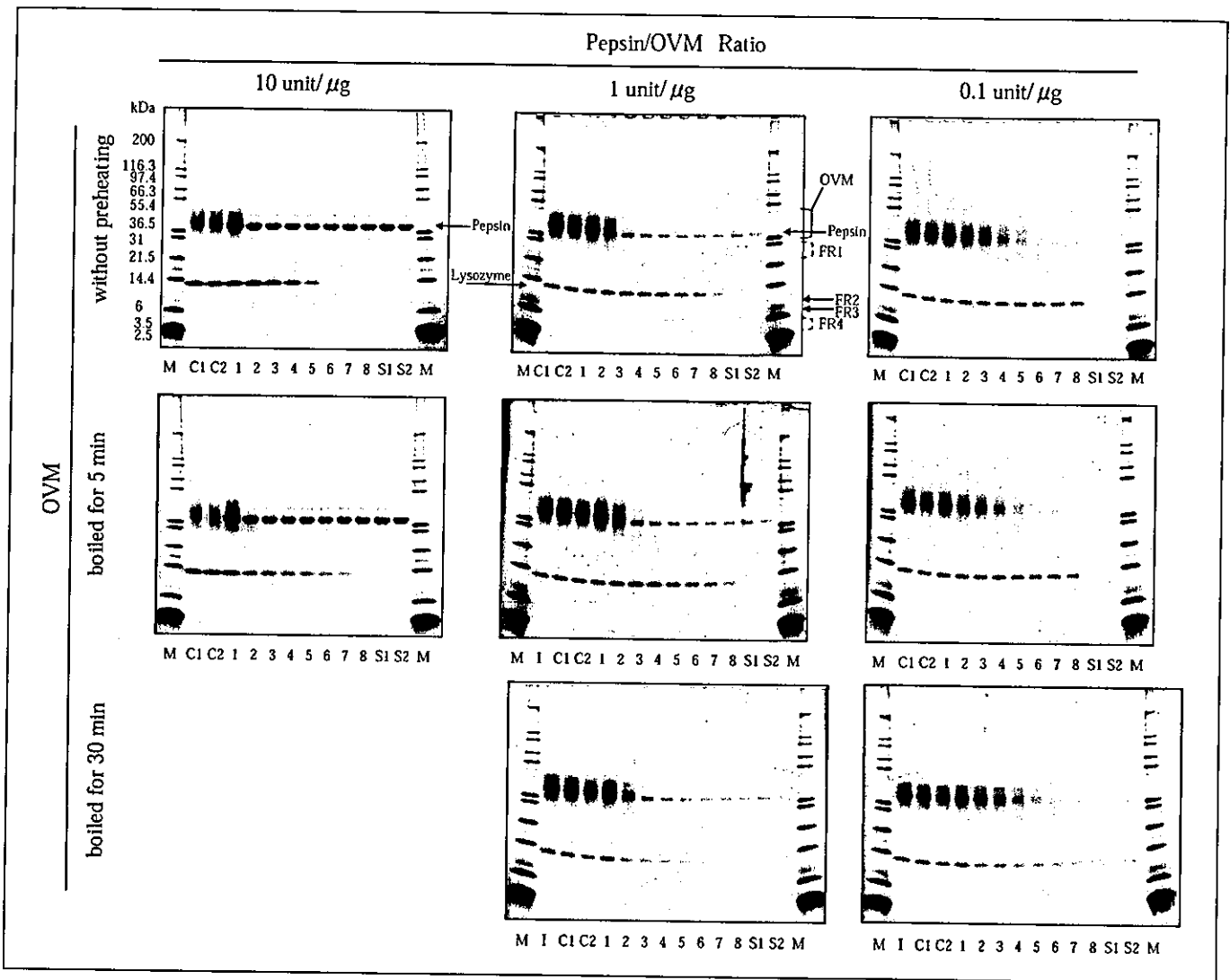


Fig. 1. Kinetic patterns of OVM digestion in SGF-containing pepsin. Digested samples were analyzed by SDS-PAGE followed by CBB staining. The digestion patterns of OVM without preheating (upper panels), preheated at 100°C for 5 min (middle panels), and preheated at 100°C for 30 min (lower panels) are shown. The ratio of pepsin to OVM was 10 unit/1 μg (left), 1 unit/1 μg (middle), and 0.1 unit/1 μg (right). Lane M = Molecular weight markers; lanes C1 and

C2 = OVM without pepsin at 0 (C1) and 60 (C2) min; lanes 1–8 = SGF-digested OVM at 0, 0.5, 2, 5, 10, 20, 30 and 60 min, respectively; lanes S1 and S2 = SGF alone at 0 (S1) and 60 (S2) min; lanes I = OVM without preheating; FR 1 = fraction 1 containing a fragment at 23.5–28.5 kDa; FR 2 = fraction 2 containing a 10-kDa fragment; FR 3 = fraction 3 containing a 7-kDa fragment; FR 4 = fraction 4 containing 4.5- to 6-kDa fragments.

Sequence Analysis of OVM Fragments

The sequences of the five N-terminal residues in each fragment were analyzed, and the data are summarized in table 1. Figure 4 schematically depicts the identified fragments; the arrows in the upper panel indicate the sites of pepsin cleavage.

The internal sequences of the FR 1, FR 3, and FR 4 fragments were also identified by LC/MS/MS and are shown in table 2 and in the upper panel of figure 4.

Reactivity of the Fragments with Serum IgE from Patients with Egg White Allergy

Western blot analysis using patient sera as the source of the primary antibodies was performed to identify sera that reacted with intact OVM and the SGF fragments. Representative blotting data are shown in figure 5, and all the results are listed in table 3. Ninety-two percent of the serum samples from allergic patients reacted with OVM, and 93% of the OVM-positive sera reacted with FR 1

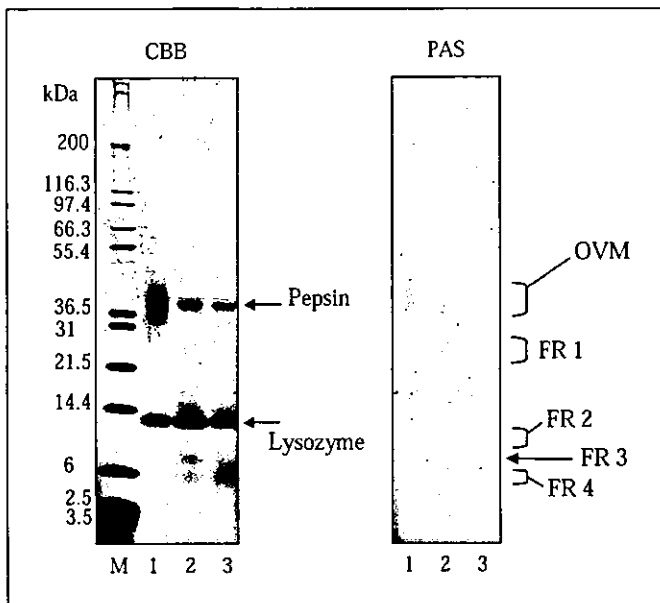


Fig. 2. CBB and PAS staining of OVM fragments following digestion in SGF (pepsin/OVM = 1 unit/ μ g) for 5 and 30 min. Lane M = Molecular weight markers; lane 1 = original OVM (2.5 μ g/lane); lanes 2 and 3 = OVM digested for 5 and 30 min, respectively, and concentrated (12 μ g, equivalent to the original OVM/lane). Samples were applied to two SDS-PAGE gels and electrophoresed. One plate (left panel) was stained with CBB reagent, and the other (right panel) was stained with PAS reagent.

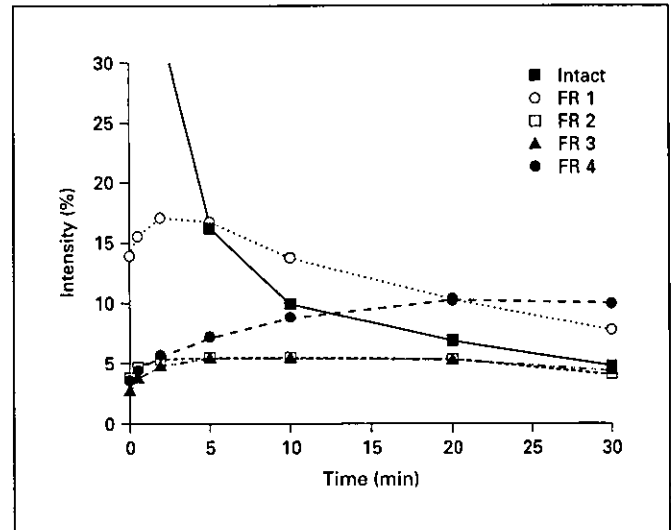


Fig. 3. Quantification of the SGF-digestion pattern of intact OVM and the digestion fragments at a pepsin/OVM ratio of 1 unit/ μ g. The intensity of each band was calculated using the ratio of the band's density to the total density of the originally detected band at $t = 0$. Values are the mean of duplicate analyses. Similar results were observed in another set of experiments.

Table 2. Identified inside sequences in pepsin- and trypsin-digested OVM

Pepsin digestion	Fraction	Residues	Sequence
5 min	FR 1	83-89	VMVLCNR
		90-103	AFNPVCGTDGVTYD
		90-112	AFNPVCGTDGVTYDNECLLCAHK
		90-122	AFNPVCGTDGVTYDNECLLCAHKVEQGASVDKR
		113-122	VEQGASVDKR
5 min	FR 3	90-112	AFNPVCGTDGVTYDNECLLCAHK
		90-122	AFNPVCGTDGVTYDNECLLCAHKVEQGASVDKR
		104-111	NECLLCAH
		104-112	NECLLCAHK
		104-121	NECLLCAHKVEQGASVDK
		104-122	NECLLCAHKVEQGASVDKR
		113-122	VEQGASVDKR
		134-159	VSVDCSEYPKPDCTAEDRPLCGSDNK
165-185	CNFCNAVVESNGTLTSLSHFGK		
30 min	FR 4	90-112	AFNPVCGTDGVTYDNECLLCAHK
		104-111	NECLLCAH
		104-112	NECLLCAHK
		104-122	NECLLCAHKVEQGASVDKR
		112-122	KVEQGASVDKR
		113-121	VEQGASVDK
		113-122	VEQGASVDKR
		165-185	CNFCNAVVESNGTLTSLSHFGK

1 11 21 31 41 51

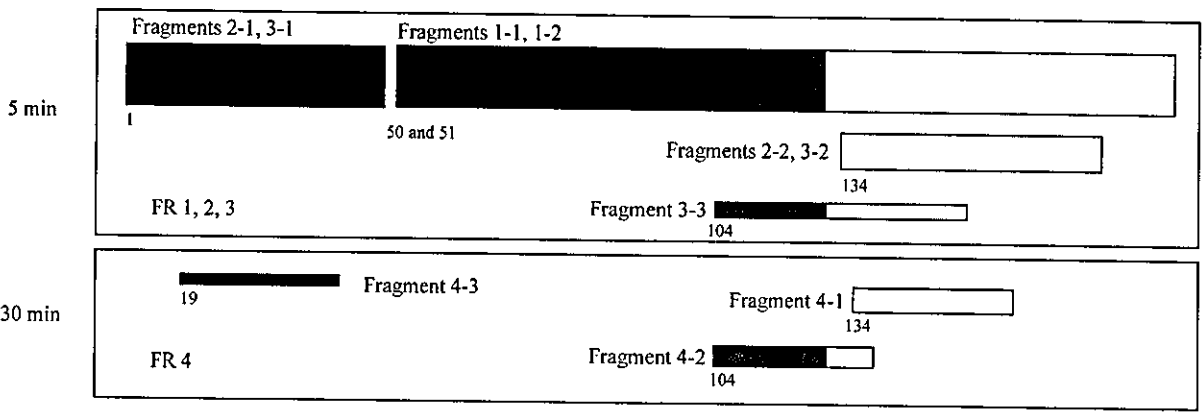
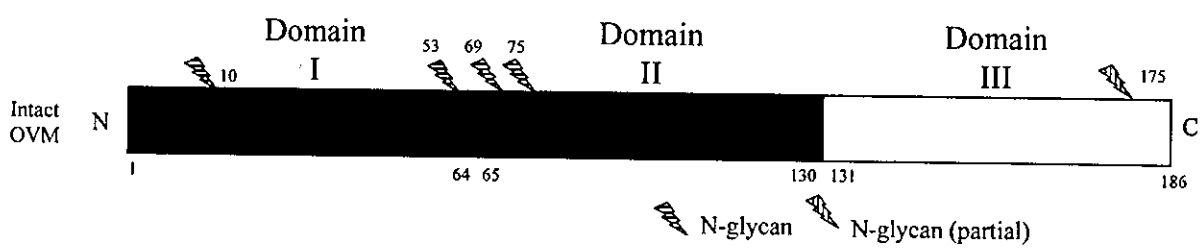
| | | | | |

1 AEVDCSRFPN ATDK**E**GKDVL VCNKDLRPIC GTDGVTYTND CLLCAYSIEF **G**TNISK**E**HDG 60

61 ECKETVPMNC SSYANTT**S**ED GKVMVLCNRA FNPVCGTDGV TYDNE**C**LLCA HKVEQGASVD 120

121 KRHDGGCRKE LA**A**V**S**VD**C**SE YPKPDCTAED RPLCGSDNKT YGNKC**N**FCNA V**V**ESNGTLTL 180

181 SHFGKC



4

after 5 min of digestion. Three of the serum samples also reacted with FR 2, FR 3, and FR 4 after 30 min of digestion.

The three samples that react with FR 2, FR 3, and FR 4 were obtained from patients who exhibited persistent allergies to egg white. One of these serum samples, No. 4, was obtained from a 3-year-old girl who is presently 6 years old; her total IgE level has decreased slightly to 4,450 IU/ml, but the specific IgE level for egg white remains at more than 100 IU/ml, and the patient has not outgrown her hypersensitivity to eggs. Another patient, No. 13, was a 1-year-old boy; 7 years later, his total and egg white-specific IgE levels had been reduced to 947 and 6.85 IU/ml, respectively, but eating raw eggs still caused allergic symptoms. The third FR 4-positive patient, No. 19, was an 11-year-old boy whose total IgE level decreased to 3,940 IU/ml and whose egg white-specific IgE decreased to 13.5 IU/ml after a period of about 2 years; however, this patient has also not outgrown his allergies. These cases and our previously reported data [17] indi-

cate that the induction of egg white tolerance may be difficult in patients whose serum IgE exhibits binding activity to digested small fragments of OVM.

Discussion

In the SGF-digestion system, preheating the OVM (100°C for 5 or 30 min) did not affect the OVM digestion pattern (fig. 1), consistent with the results of previous reports [9] in which heat treatment did not markedly decrease the allergenicity of OVM. On the other hand, a decrease in the pepsin/OVM ratio dramatically reduced the digestion rate, suggesting that digestibility may vary depending on the amount of OVM intake and the conditions of the individual's digestion system. In its native state, OVM possesses serine protease inhibitor activity. Fu et al. [11] and our group [10] previously reported that intact OVM was stable for 60 min in simulated intestinal fluid. Kovacs-Nolan et al. [15] also reported that pepsin-

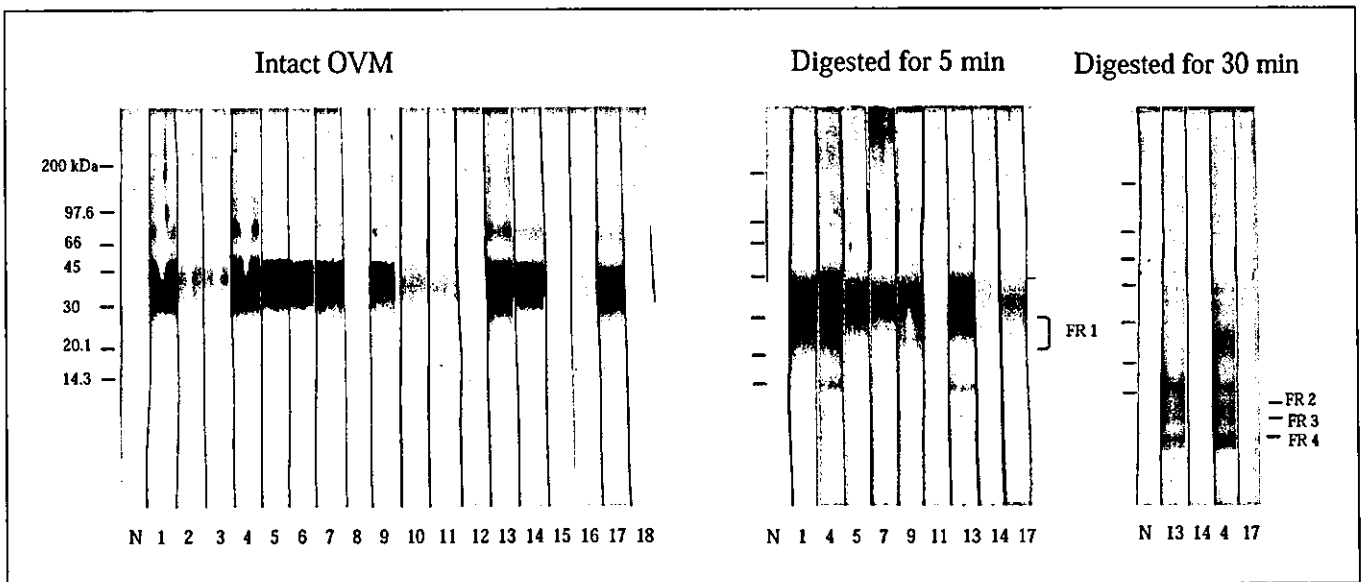


Fig. 4. Amino acid sequence and schematic representation of the SGF-digestion pattern of OVM. The amino acid sequence of OVM is shown in the upper panel. The arrows indicate the SGF-digested points according to the results of an N-terminal analysis of the OVM fragments (table 1), and the underlined regions indicate sequences identified by LC/MS/MS. Solid line = FR 1; dotted line = FR 3; dashed line = FR 4. Shaded areas represent reported human IgE epitopes [16]. The lower panel is a summary of the OVM digestion pattern according to N-terminal analysis.

Fig. 5. Western blot analysis of intact OVM and the fragments with serum IgE from egg white allergic patients and a normal volunteer. The fragments were prepared as described in the legend of figure 2. The number of each strip corresponds to the sample numbers in table 2.

Table 3. Reactivity of OVM and pepsin fragments with patient serum IgE

No.	IgE content, IU/ml		Reactivity with patient IgE ¹				
	total	egg white-specific	intact OVM	FR 1	FR 2	FR 3	FR 4
1	3,700	>100	+++	++	-	-	-
2	402	3.74	+	n.d.	n.d.	n.d.	n.d.
3	251	6.85	+	n.d.	n.d.	n.d.	n.d.
4	6,510	>100	+++	+++	+	+	++
5	2,060	>100	++	++	-	-	-
6	1,240	12.4	++	n.d.	n.d.	n.d.	n.d.
7	4,180	31.3	++	++	-	-	-
8	56	20.1	±	n.d.	n.d.	n.d.	n.d.
9	1,355	50.7	++	++	-	-	-
10	22,810	2.11	+	n.d.	n.d.	n.d.	n.d.
11	1,463	4.65	+	-	-	-	-
12	14,230	0.70-3.49	±	n.d.	n.d.	n.d.	n.d.
13	8,000	>100	+++	+++	+	+	++
14	22,490	1.05	+++	±	-	-	-
15	934	66.3	+	n.d.	n.d.	n.d.	n.d.
16	345	20.1	+	n.d.	n.d.	n.d.	n.d.
17	1,500	80	++	+	-	-	-
18	3,300	>10	-	n.d.	n.d.	n.d.	n.d.
19	20,500	26.8	+++	++	±	±	±
20	138	45.4	++	+	-	-	-
21	940	2.44	+	+	-	-	-
22	91	0.70-3.49	+	±	-	-	-
23	828	0.9	++	+	-	-	-
24	21	3.50-17.4	-	n.d.	n.d.	n.d.	n.d.
	positive/tested		22/24 (92%) ²	13/14 (93%) ³	3/14 (21%) ³	3/14 (21%) ³	3/14 (21%) ³

n.d. = Not done.

¹ Intensity of the reactivity of each band was evaluated by the ratio to normal serum: - = <1; ± = 1-2; + = 2-5; ++ = 5-10; +++ = >10.² Percent of egg white-positive samples.³ Percent of intact OVM-positive samples.

digested OVM retains its trypsin inhibitor activity. Therefore, OVM and its pepsin-digested fragments were thought to be stable in the small intestine.

At a pepsin/OVM ratio of 1 unit/μg, FR 1 reached a maximum level after 2 min of digestion, while both FR 2 and FR 3 reached maximum levels after 5 min of digestion; thereafter, FR 1, FR 2, and FR 3 gradually decreased. However, FR 4 increased continuously throughout the 30-min period of digestion and the major fragments were seen after 30 min of digestion (fig. 3). FR 4 was mainly composed of three fragments whose N-terminals were 134V, 104N and 19V (table 1). A C-terminal sequence, 165N-185C, was also identified in FR 4 (table 2). These fragments contain known IgE epitopes [19] and therefore may cause allergic responses. Three of the

OVM-positive sera from patients with egg white allergy reacted positively with the FR 4 fragments (table 3).

The present results are consistent with the previous finding that pediatric subjects with a higher IgE-binding activity to pepsin-treated OVM were unlikely to outgrow their egg allergy [17]. For peanut allergies, differences in IgE-binding epitopes have been reported between the patients with clinically active peanut allergies and those who developed a tolerance, regardless of the presence of high or low peanut-specific IgE levels [20].

The N-terminal residue of the major fragment (4-1) of FR 4 was Val-134 (30%; table 1). This fragment retains most of domain III, which has been reported to have significantly higher human IgG- and IgE-binding activities than those of domains I and II [12]. A domain-III OVM

variant has also been reported to cause a reduction in immunogenicity and allergenicity [21].

Domains I, II, and III contain one, three, and one N-glycosylation sites, respectively [7]. The possible relation between the carbohydrate chain in domain III and allergenicity is interesting. One report suggested that this carbohydrate chain may play an important role in allergenic determinants against human IgE antibody [13], and another report suggested that the carbohydrate chains of OVM may protect against peptic hydrolysis [22]. However, the carbohydrate moieties have been shown to have only a minor effect on allergenicity [23]. As shown in figure 2, intact OVM, FR 1, and FR 2 fragments were detected using PAS staining, suggesting the presence of carbohydrate chains, but FR 4 was not stained with the PAS reagent, despite being clearly detected with CBB. Therefore, FR 4 might contain little or no carbohydrate chains. Since FR 4 seems to maintain its allergenic potential, as described above, the absence of the carbohydrate chains in FR 4 suggests that they are not necessary for OVM allergenicity. Since the minimum peptide size capable of eliciting significant clinical symptoms of allergic reactions is thought to be 3.1 kDa [24], FR 4 may be able to trigger mast cell activation and elicit clinical symptoms.

In this report, the SGF-digestion kinetic pattern of OVM was investigated in detail, and the partial sequences

of the fragments in the 4 fractions separated by SDS-PAGE were determined. Furthermore, the reactivity of the fragments with a number of serum samples from patients with egg white allergies was detected using Western blotting. The four fractions were separated according to their molecular weight and consisted of more than one fragment, as determined by N-terminal analysis. The identified sequences that started at Asn-104 and Val-134 in FR 3, as determined using LC/MS/MS (table 2), coincided with the 3-2 and 3-3 fragments in the N-terminal analysis (table 1), and the sequence that started at Asn-104 in FR 4 coincided with fragment 4-2. Moreover, the LC/MS/MS analysis indicated that FR 3 and FR 4 contained other parts of domain II and the C-terminal sequence N165-C185, which are thought to be minor components of these fractions. The combination of SGF digestion and patient IgE may provide useful information for the diagnosis and prediction of potential OVM allergenicity.

Acknowledgement

This study was supported by a grant from the Ministry of Health, Labor and Welfare, and the Cooperative System for Supporting Priority Research of Japan Science and Technology Agency.

References

- 1 Sampson HA, McCaskill CC: Food hypersensitivity and atopic dermatitis: Evaluation of 113 patients. *J Pediatr* 1985;107:669-675.
- 2 Bock SA, Sampson HA, Atkins FM, Zeiger RS, Lehrer S, Sachs M, Bush RK, Metcalfe DD: Double-blind, placebo-controlled food challenge (DBPCFC) as an office procedure: A manual. *J Allergy Clin Immunol* 1988;82:986-997.
- 3 Bock SA, Atkins FM: Patterns of food hypersensitivity during sixteen years of double-blind, placebo-controlled food challenges. *J Pediatr* 1990;117:561-567.
- 4 Boyano-Martinez T, Garcia-Ara C, Diaz-Pena JM, Martin-Esteban M: Prediction of tolerance on the basis of quantification of egg white-specific IgE antibodies in children with egg allergy. *J Allergy Clin Immunol* 2002;110:304-309.
- 5 Kotaniemi-Syrjanen A, Reijonen TM, Rompanen J, Korhonen K, Savolainen K, Korppi M: Allergen-specific immunoglobulin E antibodies in wheezing infants: The risk for asthma in later childhood. *Pediatrics* 2003;111:e255-e261.
- 6 Li-Chan E, Nakai S: Biochemical basis for the properties of egg white. *Crit Rev Poultry Biol* 1989;2:21-58.
- 7 Kato I, Schrode J, William J, Kohr WJ, Laskowski M Jr: Chicken ovomucoid: Determination of its amino acid sequence, determination of the trypsin reactive site, and preparation of all three of its domains. *Biochemistry* 1987;26:193-201.
- 8 Matsuda T, Watanabe K, Nakamura R: Immunological and physical properties of peptic-digested ovomucoid. *J Agric Food Chem* 1983;31:942-946.
- 9 Honma K, Aoyagi M, Saito K, Nishimuta T, Sugimoto K, Tsunoo H, Niimi H, Kohno Y: Antigenic determinants on ovalbumin and ovomucoid: Comparison of the specificity of IgG and IgE antibodies. *Arerugi* 1991;40:1167-1175.
- 10 Takagi K, Teshima R, Okunuki H, Sawada J: Comparative study of in vitro digestibility of food proteins and effect of preheating on the digestion. *Biol Pharm Bull* 2003;26:969-973.
- 11 Fu TJ, Abbott UR, Hatzos C: Digestibility of food allergens and nonallergenic proteins in simulated gastric fluid and simulated intestinal fluid—a comparative study. *J Agric Food Chem* 2002;50:7154-7160.
- 12 Zhang JW, Mine Y: Characterization of IgE and IgG epitopes on ovomucoid using egg-white-allergic patients' sera. *Biochem Biophys Res Commun* 1998;253:124-127.
- 13 Matsuda T, Nakamura R, Nakashima I, Hasegawa Y, Shimokata K: Human IgE antibody to the carbohydrate-containing third domain of chicken ovomucoid. *Biochem Biophys Res Commun* 1985;129:505-510.
- 14 Thomas K, Aalbers M, Bannon GA, Bartels M, Dearman RJ, Esdaile DJ, Fu TJ, Glatt CM, Hadfield N, Hatzos C, Hefle SL, Heylings JR, Goodman RE, Henry B, Herouet C, Holsapple M, Ladics GS, Landry TD, MacIntosh SC, Rice EA, Privalle LS, Steiner HY, Teshima R, Van Ree R, Woolhiser M, Zawodny J: A multi-laboratory evaluation of a common in vitro pepsin digestion assay protocol used in assessing the safety of novel proteins. *Regul Toxicol Pharmacol* 2004;39:87-98.

- 15 Kovacs-Nolan J, Zhang JW, Hayakawa S, Mine Y: Immunochemical and structural analysis of pepsin-digested egg white ovomucoid. *J Agric Food Chem* 2000;48:6261–6266.
- 16 Besler M, Petersen A, Steinhart H, Paschke A: Identification of IgE-Binding Peptides Derived from Chemical and Enzymatic Cleavage of Ovomucoid (Gal d 1). Internet Symposium on Food Allergens 1999;1:1–12. <http://www.food-allergens.de>
- 17 Urisu A, Yamada K, Tokuda R, Ando H, Wada E, Kondo Y, Morita Y: Clinical significance of IgE-binding activity to enzymatic digests of ovomucoid in the diagnosis and the prediction of the outgrowing of egg white hypersensitivity. *Int Arch Allergy Immunol* 1999; 120:192–198.
- 18 Zacharius RM, Zell TE, Morrison JH, Woodlock JJ: Glycoprotein staining following electrophoresis on acrylamide gels. *Anal Biochem* 1969;30:148–152.
- 19 Mine Y, Zhang JW: Identification and fine mapping of IgG and IgE epitopes in ovomucoid. *Biochem Biophys Res Commun* 2002; 292:1070–1074.
- 20 Beyer K, Ellman-Grunther L, Jarvinen KM, Wood RA, Hourihane J, Sampson HA: Measurement of peptide-specific IgE as an additional tool in identifying patients with clinical reactivity to peanuts. *J Allergy Clin Immunol* 2003;112:202–207.
- 21 Mine Y, Sasaki E, Zhang JW: Reduction of antigenicity and allergenicity of genetically modified egg white allergen, ovomucoid third domain. *Biochem Biophys Res Commun* 2003; 302:133–137.
- 22 Matsuda T, Gu J, Tsuruta K, Nakamura R: Immunoreactive glycopeptides separated from peptic hydrolysate of chicken egg white ovomucoid. *J Food Sci* 1985;50:592–594.
- 23 Cooke SK, Sampson HA: Allergenic properties of ovomucoid in man. *J Immunol* 1997;159: 2026–2032.
- 24 Kane PM, Holowka D, Baird B: Cross-linking of IgE receptor complexes by rigid bivalent antigens greater than 200 Å in length triggers cellular degranulation. *J Cell Biol* 1988;107: 969–980.

Improved sensitivity for insulin in matrix-assisted laser desorption/ionization time-of-flight mass spectrometry by premixing α -cyano-4-hydroxycinnamic acid matrix with transferrin

Tetsu Kobayashi*, Hiroshi Kawai, Takuo Suzuki, Toru Kawanishi and Takao Hayakawa

Division of Biological Chemistry and Biologicals, National Institute of Health Sciences, 1-18-1 Kamiyoga, Setagaya-ku, Tokyo 158-8501, Japan

Received 27 February 2004; Revised 25 March 2004; Accepted 25 March 2004

This report describes an enhancement of the signal intensities of proteins and peptides in matrix-assisted laser desorption/ionization time-of-flight mass spectrometry (MALDI-TOFMS). When α -cyano-4-hydroxycinnamic acid (CHCA) premixed with human transferrin (Tf) was used as a matrix, the signal intensity of insulin was amplified to more than ten times that of the respective control in CHCA without Tf. The detection limit of insulin was 0.39 fmol on-probe in the presence of Tf, while it was 6.3 fmol in the absence of Tf. The signal intensity of insulin was also enhanced when the CHCA matrix was premixed with proteins other than Tf (80 kDa), such as horse ferritin (20 kDa), bovine serum albumin (BSA, 66 kDa), or human immunoglobulin G (150 kDa). The optimum spectrum of insulin was obtained when the added amount of protein was in the range 0.26–0.62 pmol, regardless of the molecular weight of the added protein. Tf and BSA outperformed the other tested proteins, as determined by improvements in the resulting spectra. When the mass spectra of several peptides and proteins were recorded in the presence of Tf or BSA, the signal intensities of large peptides such as glucagon were enhanced, though those of smaller peptides were not enhanced. In addition, the signal enhancement achieved with Tf and BSA was more pronounced for the proteins, including cytochrome C, than for the large peptides. This enhancement effect could be applied to improve the sensitivity of MALDI-TOFMS to large peptides and proteins. Copyright © 2004 John Wiley & Sons, Ltd.

Matrix-assisted laser desorption/ionization time-of-flight mass spectrometry (MALDI-TOFMS) and electrospray ionization mass spectrometry have been widely used in studies of protein chemistry, including proteomics studies aimed at sequence identification or quantitative analyses following enzymatic digestion by isotope-coded affinity tags and other tagging systems.^{1–8} In particular, MALDI-TOFMS has been used for the qualitative and quantitative analysis of intact proteins.^{9–11} When the MALDI technique was first introduced as an ionization method for proteins, a mixture of fine metal powder and glycerol, or nicotinic acid, was used as the matrix.^{12,13} Progress has been made with other matrix materials such as sinapinic acid, 2,5-dihydroxybenzoic acid (DHB), and α -cyano-4-hydroxycinnamic acid (CHCA), which have some desirable properties such as less intense adduct peaks and a relative insensitivity to contamination.^{14–16} With the MALDI approach, analyte proteins are dispersed on a surface in a thin layer of matrix. The energy of an incident

pulse of laser photons is absorbed by the matrix to form a jet of matrix vapor that lifts the analyte proteins from the surface and transforms some of them into ions.¹³

However, the mechanisms by which laser light irradiation is able to generate macromolecular ions have not been fully verified to date. It has been reported that the ionization of macromolecules by the MALDI process is affected by several factors. For example, peptide signal intensity was increased by the use of acetone as the solvent for CHCA matrix instead of employing the commonly used solvent, a mixture of acetonitrile and aqueous 0.1% trifluoroacetic acid (TFA).¹⁷ The signal-to-noise (S/N) ratios for macromolecules are low in DHB matrix, but the addition of suitable additives (fructose, glucose, fucose, or 2-hydroxy-5-methoxybenzoic acid) to the DHB matrix improved its performance in the high molecular mass range.^{18–21} In the CHCA and sinapinic acid matrices, the detection of higher molecular weight proteins was improved by using polytetrafluoroethylene (Teflon) as sample support.^{22,23}

Recently, we investigated a method of identifying and quantifying proteins in blood using mass spectrometry. During the present study, we discovered that the signal intensity of human insulin was augmented more than 10-fold when transferrin (Tf) was mixed with the CHCA matrix

*Correspondence to: T. Kobayashi, Division of Biological Chemistry and Biologicals, National Institute of Health Sciences, 1-18-1 Kamiyoga, Setagaya-ku, Tokyo 158-8501, Japan.
E-mail: kobayash@nihs.go.jp
Contract/grant sponsor: Ministry of Health, Labor and Welfare, Japan.

solution used for MALDI-TOFMS. This phenomenon was not specific to either insulin or Tf, which suggested that such enhancements could be used more generally to improve the sensitivity of protein analysis with MALDI-TOFMS.

EXPERIMENTAL

Materials

Human atrial natriuretic peptide (hANP), glucagon, insulin, insulin-like growth factor-1 (IGF-1), transferrin (Tf), bovine serum albumin (BSA), horse spleen ferritin (106 mg/mL in 0.15 M NaCl), and ProteoMass Peptide & Protein, were purchased from Sigma (St. Louis, MO, USA). Human immunoglobulin G (IgG, 11.3 mg/mL in 0.01 M sodium phosphate, 0.5 M NaCl, pH 7.6) was obtained from Wako Pure Chemical Industries Ltd. (Tokyo, Japan). Human insulin, IGF-1, glucagon, and hANP stock solutions were prepared at concentrations of 100 pmol/ μ L by dissolving them in 0.1% TFA. Tf and BSA stock solutions were prepared at concentrations of 10 mg/mL by dissolving the materials in Millipore deionized water. ProteoMass Peptide & Protein stock solutions, which include bradykinin fragment 1-7, human angiotensin II, synthetic peptide P₁₄R, human ACTH fragment 18-39, bovine insulin oxidized B chain, bovine insulin, equine cytochrome C, equine apomyoglobin, rabbit aldolase, and BSA, were prepared at concentrations of 100 pmol/ μ L each, according to the manufacturer's instructions.

Sample application and data acquisition

The Tf-mixed CHCA was a 5:1 mixture of the CHCA solution (10 mg/mL in 50% acetonitrile in 0.1% aqueous TFA) and Tf solution (0.10 μ g/ μ L; the final concentration was approximately 8.3 ng/ μ L), corresponding to 0.21 pmol Tf on each well of the target plate, if not otherwise noted. The control CHCA was a mixture of the CHCA solution and deionized water (5:1). A portion of each sample solution was immediately mixed with an equal volume of the matrix solution with or without Tf, and an aliquot of 2 μ L (corresponding to 1 μ L of sample solution) was applied to a stainless steel target plate. Mass spectrometric analyses were performed using an AB4700 proteomics analyzer (Applied Biosystems, Foster, CA, USA). The operating conditions were as follows: Nd:YAG laser (355 nm), linear mode, and detection of positive ions. The spectra were generated by signal averaging 50 laser shots into a single spectrum. The signal intensity was obtained after performing background correction and noise reduction using the Data Processor software (Applied Biosystems). This software was also used to determine the detection limit.

To confirm whether or not the matrix solution was at an optimum composition, serially diluted CHCA, DHB, or sinapinic acid solutions (from 10 to 0.078 mg/mL in 50% acetonitrile, 50% 0.1% TFA) were added to the insulin solution (100 fmol/ μ L). The most intense signal was obtained when 10 mg/mL CHCA was added to the insulin solution.

RESULTS AND DISCUSSION

Human insulin solution (6.3 fmol/ μ L) was mixed with an equal volume of Tf-mixed CHCA or control CHCA. When

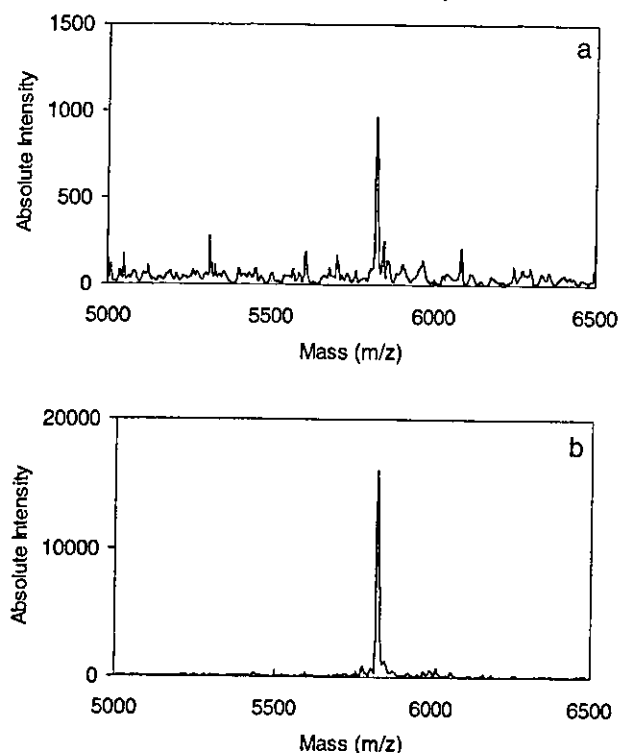


Figure 1. MALDI mass spectra of human insulin. The insulin solution (6.3 fmol/ μ L) and matrix solution were mixed together in equal volumes; 2 μ L of the resulting mixture were applied to a target plate, allowed to dry, and analyzed by MALDI-TOFMS (see Experimental). The matrix solution was a 5:1 mixture of CHCA solution (10 mg/mL in 50% acetonitrile in 0.1% aqueous TFA) with deionized water or Tf solution (0.10 μ g/ μ L). (a) Control CHCA used as matrix. (b) Tf-mixed CHCA used as matrix.

the Tf-mixed CHCA was used as matrix, the signal intensity of insulin in the MALDI-TOFMS detection system was amplified more than 10-fold relative to that achieved with the control CHCA (Fig. 1). To assess the sensitivity of insulin detection, the matrix solution was added to serially diluted insulin solutions (from 100 to 0.20 fmol/ μ L in deionized water), and samples were then spotted on a target plate. The detection limit of insulin was 0.39 fmol on the target plate in a Tf-mixed CHCA matrix under the present experimental conditions, whereas this limit was 6.3 fmol in the case of CHCA without Tf (Fig. 2).

To obtain the optimum concentration of Tf for the enhancement of insulin measurement sensitivity, the CHCA solution was mixed with serially diluted Tf solutions (from 1.0 μ g/ μ L to 7.8 ng/ μ L) before addition to the insulin solution (100 fmol/ μ L). The signal intensity increased in a Tf-concentration-dependent manner (Fig. 3(a)). However, the S/N ratio decreased when the Tf concentration was more than 125 ng/ μ L (Fig. 3(b)), though it should be noted that the S/N value was still higher than the corresponding control value, i.e., 15 ± 7 . A signal for 0.39 fmol/ μ L insulin was detected in the CHCA solution mixed with 0.1 μ g/ μ L Tf (Fig. 2), whereas the signal for 1.6 fmol/ μ L insulin was not detected in the CHCA solution mixed with 1.0 μ g/ μ L Tf (data not shown). These results suggest that the detection limit was also decreased in the presence of a high concentration of Tf.

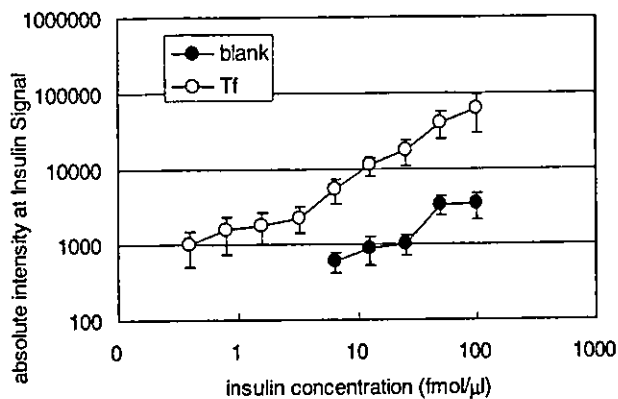


Figure 2. Dependence of insulin signals on insulin concentration. Sequentially diluted human insulin solution (100 to 0.20 fmol/μL in deionized water) and matrix solution were mixed in equal volumes. The matrix solution was a 5:1 mixture of the CHCA solution with either deionized water or Tf solution (0.10 μg/μL). The absolute intensity of the insulin signal obtained from Tf-mixed CHCA (open circles) is compared with that obtained for the control CHCA (closed circles). Each point represents the mean ± S.E. of four tests.

It is known that an excess amount of protein components can strongly influence the behavior of the MALDI process, resulting in partial or complete ion signal suppression.²⁴ In addition, the optimum mass ratio between the analyte and matrix for MALDI analysis has been demonstrated empiri-

cally.¹⁵ When the CHCA was mixed with 1.0 μg/μL Tf, the excess amount of Tf might have suppressed the signal intensity of insulin as well. However, if that amount is appropriate, Tf appears somehow capable of enhancing the signal.

To determine whether or not the enhancement of the insulin MALDI-TOFMS signal intensity was specific to Tf, the CHCA solution was mixed with serially diluted solutions of several peptides and proteins before its addition to the insulin solution. The insulin signal intensity was also enhanced in the presence of ferritin (20 kDa), BSA (66 kDa), or IgG (150 kDa) (Fig. 4(a)). However, this was not found to occur in a simple concentration-dependent manner in the case of either ferritin or IgG; furthermore, when the CHCA solution was mixed with more than 2.0 μg/μL of these protein solutions, no insulin signal was detected. The enhancement of the insulin signal intensity was relatively small in the presence of peptides such as hANP (3.1 kDa) and glucagon (3.4 kDa). In addition, when the CHCA solution was mixed with more than 77 ng/μL of hANP or 87 ng/μL of glucagon, no insulin signal was detected. Among the tested peptides and proteins, the insulin signal intensity was enhanced most effectively in the presence of Tf (80 kDa) or BSA. Therefore, it is probable that this type of enhancement requires an added protein of moderate molecular weight, namely 66–80 kDa.

With regard to the results for the serial dilutions of the added peptides and proteins, the highest S/N values were obtained at 4.8 ng/μL hANP, 5.4 ng/μL glucagon, 66 ng/μL ferritin, 0.13 μg/μL BSA, 0.13 μg/μL Tf, or 0.57 μg/μL

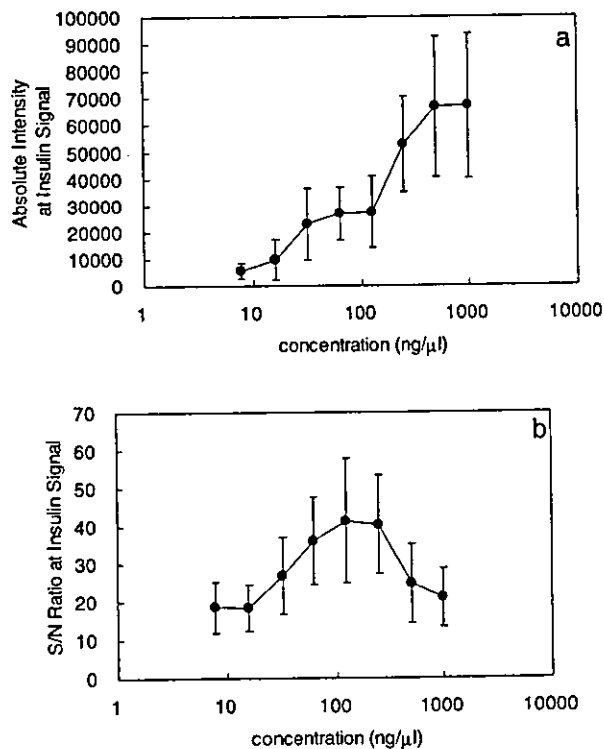


Figure 3. Dependence of insulin signal on Tf concentration. Serially diluted Tf solution was added to five volumes of the CHCA solution before mixing the resulting solution with an equal volume of human insulin (100 fmol/μL): (a) absolute intensity (arbitrary units) and (b) S/N ratio of the insulin signal in the MALDI analysis. Each point represents the mean ± S.E. of four tests.

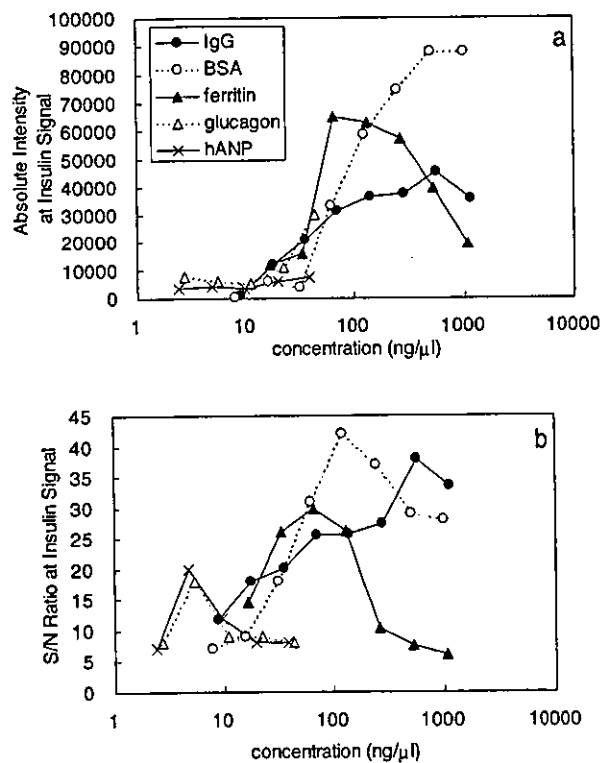


Figure 4. Dependence of insulin signal on concentrations of various added proteins. Serially diluted IgG, BSA, ferritin, glucagon, or hANP solution was added to the CHCA solution before the solution was mixed with the human insulin solution (100 fmol/μL): (a) absolute intensity (units) and (b) S/N ratio of the insulin signal. Each point represents the average of duplicate samples.

IgG (Figs. 3(b) and 4(b)), which correspond to 0.26 pmol, 0.26 pmol, 0.50 pmol, 0.32 pmol, 0.26 pmol, and 0.62 pmol, respectively, in each well. Thus, the optimum molar concentrations occurred in the same scale order, although the optimum mass concentrations of polypeptides required to enhance the signal differed markedly between the proteins and small peptides. In addition, the molar concentrations of excess peptides or proteins required to suppress the insulin signal were also found to exhibit the same scale in the same order. The ionization of insulin appeared to depend on the molar concentration of the peptide or protein which was mixed with the CHCA matrix solution.

To examine whether or not the signal enhancement was specific to human insulin, the CHCA solution premixed with Tf or BSA (0.10 µg/µL) was added to a solution of peptides and proteins, which included hANP, glucagon, human insulin, IGF-I, and ProteoMass Peptide & Protein at concentrations of 50 fmol/µL each. The signal intensities of [angiotensin II]⁺ (1046 Da), [synthetic peptide P₁₄R]⁺ (1534 Da), and [ACTH fragment]⁺ (2465 Da) were either not enhanced or were reduced in the matrix premixed with Tf or BSA (Table 1). However, the signal intensities of [hANP]⁺ (3080 Da), [glucagon]⁺ (3483 Da), [insulin B chain]⁺ (3494 Da), and [bovine insulin]⁺ (5730 Da) were enhanced as well as that of [human insulin]⁺ (5808 Da) (Table 1, Fig. 5). The signal intensities of [IGF-I]⁺ (7649 Da), [cytochrome C]⁺ (12 362 Da), and [cytochrome C]²⁺ were enhanced more than that of human insulin in the presence of Tf or BSA. In addition, the signals of [apomyoglobin]⁺ (16 952 Da) and [apomyoglobin]²⁺ were clearly observed in the presence of Tf or BSA, although their signals were not detected in the control matrix. In this latter case, the signal of [apomyoglobin]⁺ overlapped with that of BSA, but not of Tf; therefore, it was more advantageous to use Tf than BSA for detecting this signal. Since BSA was included in the ProteoMass Peptide & Protein solution, the signals of [BSA]⁺ (66 430 Da), [BSA]²⁺, [BSA]³⁺, and [BSA]⁴⁺ were also detected in the presence of Tf (Table 1, Fig. 5(b)).

The results reported above demonstrate that the enhancement of the signal intensity achieved with the use of Tf and

BSA was observed for both peptides and proteins, and this effect was not specific to human insulin. The degree of enhancement was dependent on the molecular weights of the peptides and proteins, and no such enhancement was observed in the case of small peptides; in this regard a dividing line appeared to exist between [ACTH fragment]⁺ (2465 Da) and [hANP]⁺ (3080 Da).

The mechanism by which signal intensity enhancement was achieved with the use of peptides and proteins mixed with the matrix solution remains unclear. However, when super DHB (a co-matrix of DHB and 2-hydroxy-5-methoxybenzoic acid) was used as the matrix, ion yields and S/N ratio improved, especially for the high-mass range.²⁰ It has been suggested that this signal enhancement was caused by a disorder in the DHB lattice, allowing 'softer' desorption. This type of signal enhancement has also been observed in the case of substance P in CHCA after fast evaporation of an acetone solvent, which resulted in the more homogeneous distribution of matrix and analytes.¹⁸ In addition, better mass resolution has been observed in the spectra of cytochrome C in a CHCA matrix desorbed from polyethylene and polypropylene membranes than has been observed with a CHCA matrix desorbed from stainless steel; it was thus suggested that such improved resolution might be due at least in part to the formation of relatively small matrix crystals within the membrane lattice structure.²⁵ In the present study, Tf and other proteins might have led to a similar disorganization in the CHCA lattice, resulting in the homogeneous distribution of insulin in the CHCA. However, the mechanism may differ from that suggested here, since the disorder in the CHCA lattice cannot reasonably account for why both Tf and BSA were able to enhance the insulin signal more effectively than either hANP or glucagon. As the next step, we are now planning to compare the crystals of the additive macromolecules plus matrix with those of the control matrix, using microscopic examination, to help elucidate the enhancement mechanism. We also intend to investigate whether the enhancement effect is observed in matrices other than CHCA. If crystallization is important,

Table 1. Signal intensities for proteins and peptides obtained using a matrix premixed with deionized water or with solutions of Tf or BSA

	Water	Tf	BSA
[Angiotensin II] ⁺	27 834 ± 10 757	17 057 ± 5021	19 755 ± 11 237
[P14R] ⁺	41 689 ± 15 289	30 675 ± 8588	29 237 ± 13 330
[ACTH 18–39] ⁺	4371 ± 1586	3801 ± 2246	5458 ± 3826
[hANP] ⁺	5158 ± 1323	6889 ± 2879	9523 ± 6384
[human glucagon] ⁺	435 ± 183	674 ± 324	978 ± 566
[insulin B chain] ⁺	367 ± 257	997 ± 251	715 ± 479
[bovine insulin] ⁺	639 ± 100	6266 ± 2736	7498 ± 5331
[human insulin] ⁺	1267 ± 130	13 321 ± 5057	12 982 ± 6863
[equine cytochrome C] ²⁺	166 ± 83	5668 ± 1975	3460 ± 1442
[human IGF-I] ⁺	459 ± 81	7667 ± 1808	6263 ± 2872
[equine apomyoglobin] ²⁺	nd	2249 ± 994	2217 ± 1087
[equine cytochrome C] ⁺	114 ± 43	7629 ± 1804	4006 ± 1981
[BSA] ⁴⁺	nd	52 ± 14	2459 ± 604
[equine apomyoglobin] ⁺	nd	1347 ± 700	2090 ± 1316
[BSA] ³⁺	nd	155 ± 13	3721 ± 1426
[BSA] ²⁺	nd	114 ± 27	3624 ± 1681
[BSA] ⁺	nd	25 ± 8	634 ± 433

Each entry is the average of the most intense signals from four samples. nd: no signal was detected.

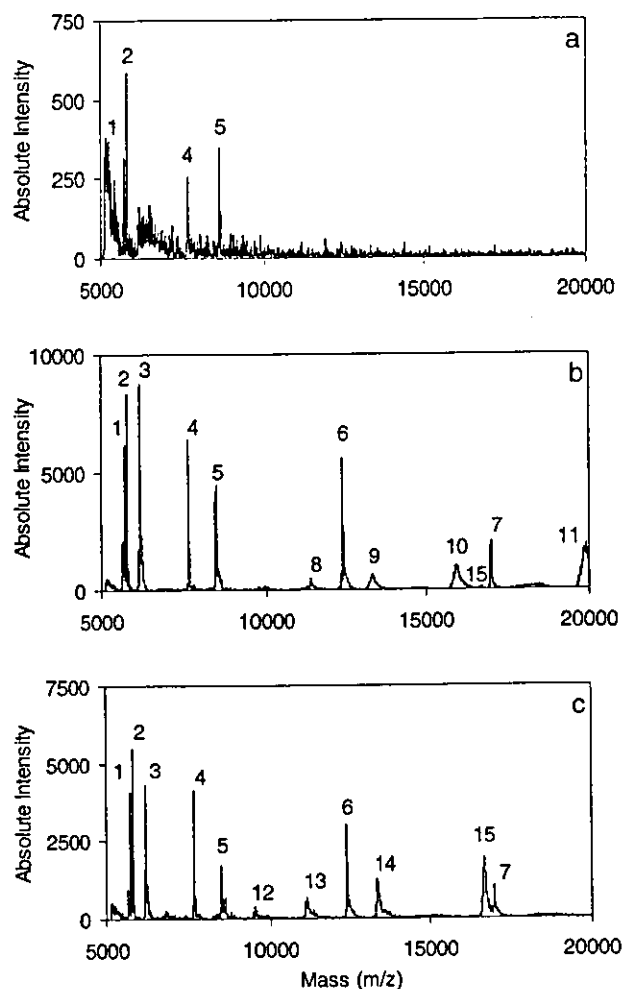


Figure 5. MALDI mass spectra of a mixture of peptides and proteins. The mixture of peptides and proteins (50 fmol/µL each) and the matrix solution were mixed together in equal volumes. The matrix solution was a 5:1 mixture of the CHCA solution with (a) deionized water; (b) Tf solution (0.10 µg/µL); and (c) BSA solution (0.10 µg/µL). Signal 1, [bovine insulin]⁺ (5730 Da); 2, [human insulin]⁺ (5808 Da); 3, [cytochrome C]²⁺; 4, [IGF-I]⁺ (7649 Da); 5, [apomyoglobin]²⁺; 6, [cytochrome C]⁺ (12 362 Da); 7, [apomyoglobin]⁺ (16 952 Da); 8, [Tf]⁷⁺; 9, [Tf]⁶⁺; 10, [Tf]⁵⁺; 11, [Tf]⁴⁺; 12, [BSA]⁷⁺; 13, [BSA]⁶⁺; 14, [BSA]⁵⁺; and 15, [BSA]⁴⁺.

the effect should not be observed when using liquid matrices.^{26,27}

The present results suggest that the enhancement brought about by either Tf or BSA could be applicable to the improvement of sensitivity in the detection of proteins by MALDI-TOFMS in general. However, when Tf or BSA was used as an enhancer in a MALDI-TOFMS system, signals from Tf and BSA were also detected, which sometimes interfered with the analysis of the target proteins. Therefore, neither Tf nor BSA appears to be the best possible enhancer. Further studies are currently underway in order to discover the best macromolecule as an enhancer.

CONCLUSIONS

We have demonstrated that the signal intensities of insulin and of several peptides and proteins were enhanced in

CHCA premixed with Tf or other peptides or proteins. The characteristics of this type of enhancement are as follows: (1) Tf (80 kDa) and BSA (66 kDa) led to better signal enhancement than did small peptides and proteins (<20 kDa) or IgG (150 kDa); (2) the optimum S/N value was observed when the added amount of peptide or protein was within the range 0.26–0.62 pmol; and (3) the signals of peptides of high molecular weight (>3000 Da) were enhanced by the addition of Tf or BSA to CHCA, although the signals of small peptides (<2500 Da) were not enhanced. This type of enhancement may be useful for the improvement of protein analyses with MALDI-TOFMS.

Acknowledgements

This study was supported in part by a research grant on Human Genome, Tissue Engineering Food Biotechnology from the Ministry of Health, Labor and Welfare, Japan.

REFERENCES

- Roberts GD, Johnson WP, Burman S, Anumula KR, Carr SA. *Anal. Chem.* 1995; **67**: 3613.
- Gygi SP, Rist B, Gerber SA, Turecek F, Gelb MH, Aebersold R. *Nat. Biotechnol.* 1999; **17**: 994.
- Münchbach M, Quadroni M, Miotto G, James P. *Anal. Chem.* 2000; **72**: 4047.
- Yao X, Freas A, Ramirez J, Demirev PA, Fenselau C. *Anal. Chem.* 2001; **73**: 2836.
- Cagney G, Emili A. *Nat. Biotechnol.* 2002; **20**: 163.
- Vogt JA, Schroer K, Hözler K, Hunzinger C, Klemm M, Biefang-Arndt K, Schillo S, Cahill MA, Schlattenholz A, Matthies H, Stegmann W. *Rapid Commun. Mass Spectrom.* 2003; **17**: 1273.
- Kuyama H, Watanabe M, Toda C, Ando E, Tanaka K, Nishimura O. *Rapid Commun. Mass Spectrom.* 2003; **17**: 1642.
- Wu SL, Choudhary G, Ramström M, Bergquist J, Hancock WS. *J. Proteome Res.* 2003; **2**: 383.
- Nakanishi T, Okamoto N, Tanaka K, Shimizu A. *Biol. Mass Spectrom.* 1994; **23**: 230.
- Nelson RW, Krone JR, Bieber AL, Williams P. *Anal. Chem.* 1995; **67**: 1153.
- Tubbs KA, Nedelkov D, Nelson RW. *Anal. Biochem.* 2001; **289**: 26.
- Tanaka K, Waki H, Ido Y, Akita S, Yoshida Y, Yoshida T. *Rapid Commun. Mass Spectrom.* 1988; **2**: 151.
- Karas M, Hillenkamp F. *Anal. Chem.* 1988; **60**: 2299.
- Beavis RC, Chait BT. *Anal. Chem.* 1990; **62**: 1836.
- Strupat K, Karas M, Hillenkamp F. *Int. J. Mass Spectrom. Ion Processes* 1991; **111**: 89.
- Beavis RC, Chaudhary T, Chait BT. *Org. Mass Spectrom.* 1992; **27**: 156.
- Vorm O, Roepstorff P, Mann M. *Anal. Chem.* 1994; **66**: 3281.
- Köstler C, Castoro JA, Wilkins CL. *J. Am. Chem. Soc.* 1992; **114**: 7572.
- Billeci TM, Stults JT. *Anal. Chem.* 1993; **65**: 1709.
- Karas M, Ehring H, Nordhoff E, Stahl B, Strupat K, Hillenkamp F, Grehl M, Krebs B. *Org. Mass Spectrom.* 1993; **28**: 1476.
- Tsarbopoulos A, Karas M, Strupat K, Pramanik BN, Nagabhushan TL, Hillenkamp F. *Anal. Chem.* 1994; **66**: 2062.
- Yuan X, Desiderio DM. *J. Mass Spectrom.* 2002; **37**: 512.
- Botting CH. *Rapid Commun. Mass Spectrom.* 2003; **17**: 598.
- Nelson RW, McLean MA. *Anal. Chem.* 1994; **66**: 1408.
- Worrall TA, Cotter RJ, Woods AS. *Anal. Chem.* 1998; **70**: 750.
- Carda-Broch S, Berthod A, Armstrong DW. *Rapid Commun. Mass Spectrom.* 2003; **17**: 553.
- Turney K, Harrison WW. *Rapid Commun. Mass Spectrom.* 2004; **18**: 629.



Analysis of site-specific glycosylation in recombinant human follistatin expressed in Chinese hamster ovary cells

Masashi Hyuga*, Satsuki Itoh, Nana Kawasaki, Miyako Ohta,
Akiko Ishii, Sumiko Hyuga, Takao Hayakawa

Division of Biological Chemistry and Biologicals, National Institute of Health Sciences, 1-18-1, Kamiyoga, Setagaya-ku, Tokyo 158-8501, Japan

Received 22 October 2003; accepted 1 April 2004

Abstract

Follistatin (FS), a glycoprotein, plays an important role in cell growth and differentiation through the neutralization of the biological activities of activins. In this study, we analyzed the glycosylation of recombinant human FS (rhFS) produced in Chinese hamster ovary cells. The results of SDS-PAGE and MALDI-TOF MS revealed the presence of both non-glycosylated and glycosylated forms. FS contains two potential *N*-glycosylation sites, Asn95 and Asn259. Using mass spectrometric peptide/glycopeptide mapping and precursor-ion scanning, we found that both *N*-glycosylation sites were partially glycosylated. Monosaccharide composition analyses suggested the linkages of fucosylated bi- and triantennary complex-type oligosaccharides on rhFS. This finding was supported by mass spectrometric oligosaccharide profiling, in which the *m/z* values and elution times of some of the oligosaccharides from rhFS were in good agreement with those of standard oligosaccharides. Site-specific glycosylation was deduced on the basis of the mass spectra of the glycopeptides. It was suggested that biantennary oligosaccharides are major oligosaccharides located at both Asn95 and Asn259, whereas the triantennary structures are present mainly at Asn95.

© 2004 The International Association for Biologicals. Published by Elsevier Ltd. All rights reserved.

Abbreviations: CHO, Chinese hamster ovary; FCS, fetal calf serum; FS, follistatin; GCC, graphitized carbon column; GnT, *N*-acetylglucosaminyl-transferase; HPAEC-PAD, high-pH anion-exchange chromatography with pulsed amperometric detection; IEF, isoelectric focusing; LC/MS, liquid chromatography/mass spectrometry; MALDI-TOF MS, matrix-assisted laser desorption/ionization time-of-flight mass spectrometry; NeuAc, *N*-acetyl neuraminic acid; NeuGc, *N*-glucoryl neuraminic acid; PNGaseF, peptide *N*-glycanase F; rhFS, recombinant human follistatin; SDS-PAGE, sodium dodecyl sulfate-polyacrylamide gel electrophoresis; TFA, trifluoroacetic acid

1. Introduction

Follistatin (FS), a glycoprotein, was first discovered in ovarian follicular fluid as an inhibitor of pituitary follicle-stimulating hormone secretion [1,2]. Subsequent studies have revealed that FS can bind to activins and neutralize their biological activities [3,4]. Activins are members of the transforming growth factor- β superfamily, and they play important roles in the regulation of cell growth and in the differentiation processes that lead to morphogenesis in early vertebrate development [5,6]. Since FS and activins are broadly distributed,

they are not confined solely to tissues associated with reproduction [7].

FS is present in heterogeneous forms [8]. The FS gene consists of 315 amino acids, and it includes six exons (Fig. 1); alternative splicing can generate two isoforms, i.e. a 315-amino-acid protein (the full-length form, FS315) and a 288-amino-acid protein (the carboxy-truncated form, FS288) [9]. The activin-neutralizing activity of FS288 is higher than that of FS315 [10,11], which appears to correlate with their heparin/heparan sulfate proteoglycan-binding abilities [12]. The heterogeneity of FS is also due to diverse glycosylation. FS has two potential *N*-glycosylation sites (Asn95 and Asn259). Oligosaccharides are generally known to play important roles in defining the properties of glycoproteins such as their biological activity, immunogenicity,

* Corresponding author. Fax: +81-3-3700-9084.

E-mail address: mhyuga@nihs.go.jp (M. Hyuga).

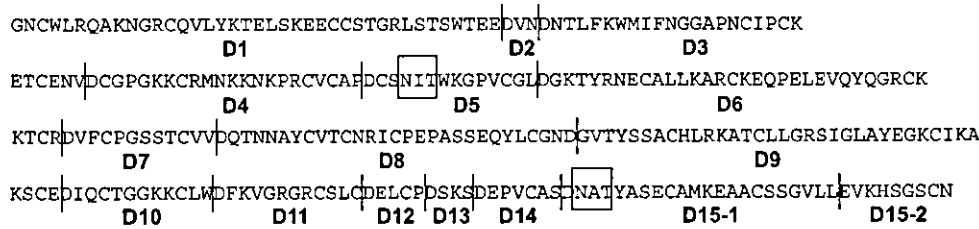


Fig. 1. Amino acid sequence of rhFS. Predicted cleavage sites with Asp-N are indicated by |. The potential *N*-glycosylation sites are indicated by boxes.

pharmacokinetics, solubility, and protease resistance [13,14]. Glycosylation on FS is also likely to exert an effect on activin-neutralizing activity; however, neither structure of the N-linked oligosaccharides in FS, nor their physiological roles, have been clarified due to the limited availability of these oligosaccharides.

The aim of this study was to elucidate the glycosylation of FS. We previously developed an oligosaccharide profiling method using liquid chromatography/mass spectrometry (LC/MS) equipped with a graphitized carbon column (GCC) [15–22]. Recently, we demonstrated a procedure for facilitating the structural analysis of glycoproteins [16]. Carbohydrate profiles and site-specific glycosylations can be characterized by the GCC-LC/MS method, followed by mass spectrometric peptide/glycopeptide mapping. We used this method to demonstrate here the carbohydrate heterogeneity and the site-specific N-linked oligosaccharide structures in recombinant human FS288 (rhFS) produced in Chinese hamster ovary (CHO) cells, in which a sufficient amount of FS could be expressed.

2. Materials and methods

2.1. Materials

Human FS315 cDNA and recombinant human activin A were kindly provided by Dr. Yuzuru Eto (Ajinomoto Co., Inc., Kawasaki, Japan). CHO cells were obtained from the Japanese Cancer Research Resources Bank (Tokyo, Japan). Mammalian expression vector pcDNA3.1/Hygro was purchased from Invitrogen (Carlsbad, CA, USA). LipofectAMINE plus reagent, Ham's F12 medium, fetal calf serum (FCS) and hygromycin were purchased from Life Technologies Inc. (Rockville, MD, USA). Pellicon XL membrane and Immobilon-P membrane were purchased from Millipore Corp. (Bedford, MA, USA). Sulfated-cellulofine was purchased from Seikagaku Corp. (Tokyo, Japan). Neuraminidase was purchased from Nakalai Tesque (Kyoto, Japan). *N*-glycosidase F (PNGaseF) and endoproteinase Asp-N (Asp-N) were purchased from Boehringer Mannheim (Mannheim, Germany). All other chemicals were obtained from commercial sources and were of the highest purity available.

2.2. Establishment of a CHO cell line expressing rhFS

Complementary DNA encoding human FS288, was constructed from FS315 cDNA, and was cloned into pcDNA3.1/Hygro. This expression vector was transfected into CHO cells with LipofectAMINE plus reagent, according to the manufacturer's instructions. To screen the transformants, the transfectants were cultured with Ham's F12 medium supplemented with 10% FCS and 1 mg/ml hygromycin. After 2 weeks, the colonies were lifted with a micropipette. Expression levels of rhFS were assessed by an activin-neutralizing assay. The candidates were cloned by limiting dilution twice and were assessed again. The most productive rhFS-expressing clone (CHO-FS) was used in the following experiments.

2.3. Preparation of rhFS

Semi-confluent CHO-FS cells were cultured in Ham's F12 medium supplemented with 2% FCS. The conditioned medium was concentrated to a 1/10 volume by filtration with a Pellicon XL membrane (M_r 5000 cut), and was applied onto a sulfated-cellulofine column (2.5×20 cm) at 2 ml/min. The column was washed with 50 mM Tris-HCl (pH 8) containing 0.5 M NaCl, and the protein was eluted with 50 mM Tris-HCl (pH 8) containing 1.5 M NaCl. The effluent from the column was fractionated, and rhFS was monitored on Western blots using polyclonal anti-FS antibody. The fractions containing rhFS were injected into an HPLC (Hitachi D7000, Hitachi Co., Tokyo, Japan) apparatus equipped with a reversed-phase column (Vydac C4, 10×300 mm, The Separations Group, Inc., Hesperia, CA, USA). The protein was eluted with a linear gradient of 16–48% of acetonitrile/0.1% trifluoroacetic acid (TFA) for 30 min at a flow rate of 2 ml/min. Elution of proteins was monitored at 280 nm and individual peaks were manually collected. Fraction of rhFS was monitored on Western blots using polyclonal anti-FS antibody.

2.4. SDS-PAGE analysis of rhFS

RhFS was digested with or without PNGaseF at 37 °C for 24 h. The proteins were separated by sodium dodecyl sulfate-polyacrylamide gel electrophoresis

(SDS-PAGE) on 10% polyacrylamide gel. The gel was stained with Coomassie blue.

2.5. Isoelectric focusing

RhFS was dissolved in 100 mM ammonium acetate buffer, pH 4.5, and incubated with neuraminidase at 37 °C for 18 h. The proteins were precipitated with cold acetone and separated by isoelectric focusing (IEF). The gel was stained with Coomassie blue.

2.6. MALDI-TOF MS

RhFS (20 µg) was subjected to positive-ion matrix-assisted laser desorption/ionization time-of-flight mass spectrometry (MALDI-TOF MS), using a Shimadzu/KRATOS MALDI I instrument (Shimadzu Co., Kyoto, Japan) with 3,5-dimethoxy-4-hydroxy-cinnamic acid as the matrix.

2.7. Monosaccharide composition analysis

Monosaccharide composition analysis was performed according to the method reported by Hardy et al. [23]. Briefly, rhFS (50 µg) was hydrolyzed with 2 M TFA at 100 °C for 3 h. Monosaccharide compositions were analyzed by high-pH anion-exchange chromatography with pulsed amperometric detection (HPAEC-PAD) using a DX-300 system (Dionex, Sunnyvale, CA, USA) equipped with a CarboPac PA-1 anion exchange column (4 × 250 mm, Dionex).

2.8. Preparation of N-linked oligosaccharides alditols

N-linked oligosaccharides alditols were prepared by a previously described method [20]. Briefly, rhFS (100 µg) was digested with 5 units of PNGaseF at 37 °C for 2 days. Proteins were precipitated with 75% cold ethanol. The oligosaccharides were incubated with NaBH₄ at room temperature for 2 h. Excess reagent was decomposed with diluted acetic acid. The mixture was applied to a Supelclean ENVI-Carb column (Supelco, Bellefonte, PA, USA), which was washed with H₂O to remove the salts. Borohydride-reduced oligosaccharides were eluted with 30% acetonitrile/5 mM ammonium acetate.

2.9. Sugar profiling by LC/MS

Sugar profiling was carried out using a MAGIC 2002 system (Michrom BioResources, Inc., Auburn, CA, USA) connected to a TSQ7000 triple-stage quadrupole mass spectrometer (ThermoFinnigan, San Jose, CA, USA) in the positive-ion mode. The column used was a GCC (Hypercarb 5 µm, 1.0 × 150 mm, ThermoFinnigan). The eluents were 5 mM ammonium acetate (pH

9.6) containing 2% acetonitrile (pump A); and 5 mM ammonium acetate (pH 9.6) containing 80% acetonitrile (pump B). The N-linked oligosaccharide alditols were eluted at a flow rate of 50 µl/min for 80 min with a gradient of 5–30% in pump B. The ESI voltage was set at 4500 V, and the capillary temperature was 175 °C. The electron multiplier was set at 1200 V.

2.10. Asp-N digestion

RhFS was reduced and S-carboxymethylated as previously described [20]. Briefly, rhFS (100 µg) was dissolved in 0.5 M Tris-HCl buffer (pH 8.6) containing 8 M guanidine and 5 mM EDTA. After reduction with 2-mercaptoethanol at room temperature for 2 h, monoiodoacetic acid was added and incubated at room temperature for 2 h in the dark. Reduced and S-carboxymethylated-rhFS (equivalent to 100 µg of rhFS) was digested with Asp-N (2 µg) in 25 mM NH₄HCO₃ (pH 8.0) at 37 °C for 20 h. The predicted peptides to be obtained by Asp-N digestion were sequentially designated as D1–D15 (Fig. 1).

2.11. Peptide/glycopeptide mapping of Asp-N-digested rhFS

Peptide/glycopeptide mapping was carried out using a MAGIC 2002 system connected to a TSQ7000 triple-stage quadrupole mass spectrometer in the positive-ion mode. The column used was a MAGIC C18 column (1.0 × 150 mm, Michrom BioResources). The eluents were 2% acetonitrile/0.05% TFA (pump A), and 80% acetonitrile/0.05% TFA (pump B). Asp-N-digested rhFS was eluted with a linear gradient from 5 to 45% in pump B at a flow rate of 50 µl/min for 40 min. The eluate was monitored at 206 nm. The ESI voltage was set at 4500 V, and the capillary temperature was 175 °C. The electron multiplier was set at 1200 V. Precursor-ion scanning was performed using argon gas as the collision gas at a pressure of 2 mTorr. The collision energy was adjusted to –25 eV. The scan rate was 3 s/scan.

3. Results

3.1. Heterogeneity of rhFS

The carbohydrate heterogeneity of rhFS was analyzed by SDS-PAGE with and without PNGaseF digestion. The intact rhFS migrated as bands of an apparent molecular mass of 32 kDa and 33–36 kDa under non-reducing conditions (Fig. 2A, lane 1). PNGaseF digestion resulted in the disappearance of the multiple bands at 33–36 kDa with increases in the 32-kDa band (Fig. 2A, lane 2). These results suggest that the 32 kDa band and higher molecular weight bands are

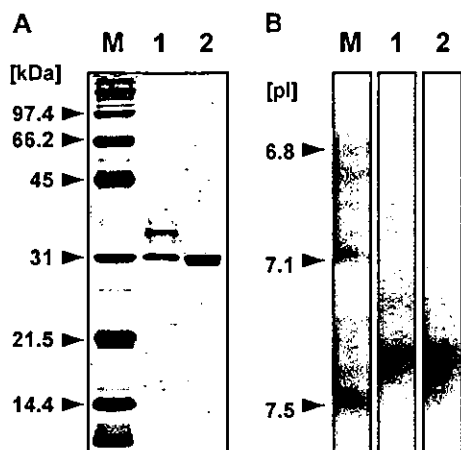


Fig. 2. (A) SDS-PAGE analysis of intact rhFS (lane 1) and PNGaseF-digested rhFS (lane 2). Lane M represents molecular weight markers. (B) IEF of intact rhFS (lane 1) and neuraminidase-digested rhFS (lane 2). Lane M represents *pI* markers.

the non-glycosylated FS and the glycosylated FS with diverse N-linked oligosaccharides, respectively.

The sialic acid heterogeneity of rhFS was analyzed by IEF with and without neuraminidase digestion. IEF of intact rhFS showed that the majority of the isoforms are located from *pI* 6.9 to 7.4 (Fig. 2B, lane 1). After treatment with neuraminidase, the acidic bands had disappeared and shifted at *pI* 7.4 (Fig. 2B, lane 2). These results suggested that the sialic acids contribute to the heterogeneity and the charge of rhFS.

The distribution of glycoforms was further investigated by MALDI-TOF MS. As shown in Fig. 3, multiple ions were detected in the range of 31.5–37 kDa. The most abundant ion at *m/z* 31,525 corresponded to the theoretical mass of non-glycosylated FS (31,514 Da). The other ions at *m/z* 33,804 and 35,600 could have

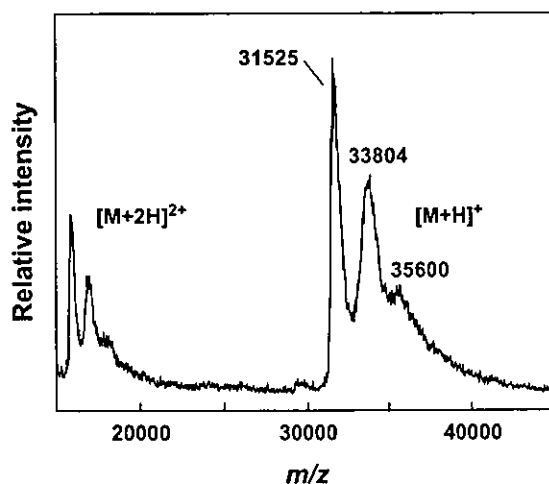


Fig. 3. MALDI-TOF MS analysis of intact rhFS. The peaks at *m/z* 31,525, 33,804 and 35,600 correspond to the non-glycosylated and glycosylated form of rhFS, respectively.

been monoglycosylated FS and diglycosylated FS, respectively.

3.2. Monosaccharide composition of rhFS

Monosaccharide composition was analyzed by hydrolysis followed by HPAEC-PAD. The relative molecular ratio of fucose and glucosamine were estimated at 1.2 and 4.4, respectively, when mannose was considered as 3.0 (Table 1). This result suggests the presence of fucosylated bi- and triantennary-type oligosaccharides. No galactosamine residue was detected, suggesting the absence of O-linked oligosaccharides.

3.3. N-linked oligosaccharides in rhFS

N-linked oligosaccharides were released from rhFS by PNGaseF digestion and reduced with NaBH₄ to avoid the separation of anomers. Then the oligosaccharide alditols from rhFS were analyzed by GCC-LC/MS. Fig. 4 shows the total ion current chromatogram of N-linked oligosaccharide alditols. The *m/z* values of intense ions observed in major peaks (peaks 8 and 12) were 1040.7²⁺ and 1186.4²⁺, which were consistent with the theoretical *m/z* values of [dHex][Hex]₅[HexNAc]₄[NeuAc]²⁺ and [dHex][Hex]₅[HexNAc]₄[NeuAc]₂²⁺, respectively (Table 2). The elution times of these oligosaccharides were in good agreement with those of fucosyl biantennary oligosaccharides bearing mono- and di-NeuAc prepared from erythropoietin, respectively [24]. An ion at *m/z* 1041.4²⁺ was also detected in peak 6. This oligosaccharide could be a sialylation isomer of peak 8 (1040.7²⁺).

Likewise, the ions at *m/z* 1790.7⁺ and 895.4²⁺ in peak 2 and at *m/z* 1077.9²⁺ in peak 3 were assigned as an asialo fucosylated biantennary oligosaccharide and an asialo fucosylated triantennary oligosaccharide, respectively. The ion at *m/z* 2389.6⁺ and 1194.6²⁺ in peak 11 was consistent with [dHex][Hex]₅[HexNAc]₄[NeuAc][NeuGc]²⁺ or [Hex]₆[HexNAc]₄[NeuAc]₂²⁺, respectively. The ions at *m/z* 2097.7⁺ and 1048.6²⁺ in peak 5 and at *m/z* 2096.5⁺ and 1049.5²⁺ in peak 8 were consistent with [dHex][Hex]₅[HexNAc]₄[NeuGc]²⁺ or [Hex]₆[HexNAc]₄[NeuAc]²⁺, respectively. The minor ions at *m/z* 1224.1²⁺, 1224.3²⁺, 1369.7²⁺, 1369.8²⁺,

Table 1
Monosaccharide composition analysis of rhFS oligosaccharides

Monosaccharide	Relative molar proportions ^a
Fucose	1.2
Galactosamine	0.3
Glucosamine	4.4
Galactose	3.2
Glucose	0.3
Mannose	3.0

^a Data are normalized to three-mannose residues.

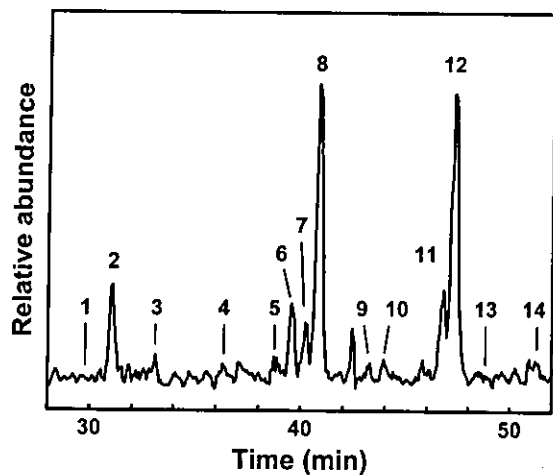


Fig. 4. Sugar map of oligosaccharide alditols released from rhFS. N-linked oligosaccharide alditols from rhFS were separated with GCC. The total ion content was scanned using the positive-ion mode at m/z 700–2400.

1370.5²⁺ and 1515.5²⁺ in peaks 7, 9, 11, 12, 13 and 14 were deduced to the fucosylated triantennary oligosaccharides with NeuAc, respectively.

The ratio of oligosaccharides was estimated as follows: fucosylated biantennary, ca. 85%, and fucosylated triantennary structures, ca. 10%, based on their ion currents; these results were in good agreement with the results of the monosaccharide composition analysis.

3.4. Site-specific glycosylation of rhFS

FS contains two potential *N*-glycosylation sites (Asn95 and Asn259, Fig. 1). The site-specific glycosylation and other post-translational modifications, such as phosphorylation and hydroxylation, were analyzed by mass spectrometric peptide/glycopeptide mapping (Fig. 5a, Table 3). Most of the non-glycosylated peptides were detected except for the small peptides, i.e. peptides D2 (tripeptide), D13 (tetrapeptide), and D12 (pentapeptide), which suggests the absence of *O*-glycans and any post-translational modifications on these peptides. The small peptides have no putative *N*-glycosylation site (Fig. 1), and no galactosamine residue was detected (Table 1). These findings suggest the absence of *N*- and *O*-linked oligosaccharides. However, the possibility remains that the small peptides are modified, such as by phosphorylation. Two unpredicted peptides (m/z 1176.2²⁺ and 510.4²⁺) were detected among the Asp-N digests of rhFS. They were assigned to peptides D15-1 and D15-2, which were produced from peptide D15 by further cleavage at the amino-terminal of Glu280. It was reported that a cleavage at the N-terminal site of glutamic acid is a possible cut site for Asp-N under the same conditions [25]. Peptides D5 and D15-1, each of which

Table 2
Putative structures of N-linked oligosaccharides deduced from the GCC-LC/MS

Peak No. ^a	Carbohydrate structure ^b	Theoretical mass ^c	Observed mass ^d		
			M ⁺	M ²⁺	M ³⁺
1		1627.5	1628.3	814.2	-
2		1789.7	1790.7	895.4	-
3		2155.0	-	1077.9	-
4		1934.7	-	967.9	-
5		2096.9	2097.7	1048.6	-
6		2080.9	2081.2	1041.4	-
7		2446.3	-	1224.1	817.4
8		2096.9	2096.5	1049.6	-
		2080.9	2082.2	1040.7	-
9		2446.3	-	1224.3	-
10		2226.0	-	1114.2	-
11		2388.2	2389.6	1194.6	-
		2737.5	-	1369.7	913.4
12		2372.2	2372.2	1186.4	-
		2737.5	-	1369.8	-
13		2737.5	-	1370.5	913.8
14		3028.8	-	1515.5	-

Note: The observed m/z of *1 and *2 are also consistent with the theoretical m/z value of [Hex]₆[HexNAc]₄[NeuAc] and [Hex]₆[HexNAc]₄[NeuAc]₂, respectively.

^a Peak label in Fig. 4.

^b Proposed structures based on molecular weight. Symbols: solid squares, GlcNAc; open circles, mannose; open diamonds, galactose; dotted diamonds, fucose; solid circle, NeuAc; dotted circle, NeuGc.

^c Calculated average mass.

^d Mass of the ion measured in the positive-ion ESI mass spectrum from alditols.

have potential glycosylation site, were detected as non-glycosylated forms in the peptide/glycopeptide map.

Precursor-ion scanning, which can detect [Hex][HexNAc]⁺ at m/z 366 produced by collision-induced dissociation, was performed for the monitoring of the glycopeptides. The TIC chromatogram of the precursor-ion scanning showed two significant peaks, peaks G1 and G2 (Fig. 5b). Fig. 6 shows the mass spectra of peaks G1 and G2 in Fig. 5b. On the basis of the theoretical masses of the peptides and oligosaccharides identified by sugar mapping (Table 2), peaks G1 and G2

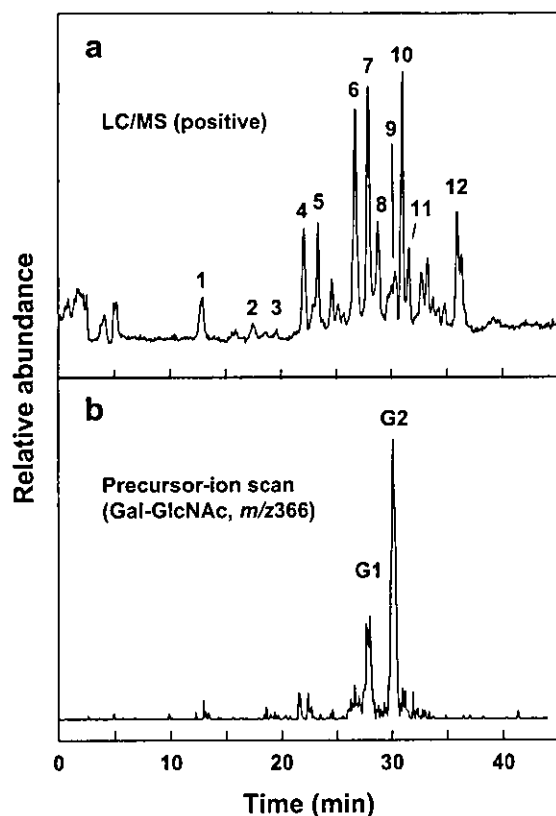


Fig. 5. Peptide/glycopeptide map of the rhFS Asp-N digest. The total ion current chromatogram of LC/MS in the positive-ion mode at m/z 400–2400 (a), and the TIC chromatogram of LC/MS/MS, precursor-ion scan of m/z 366 (b).

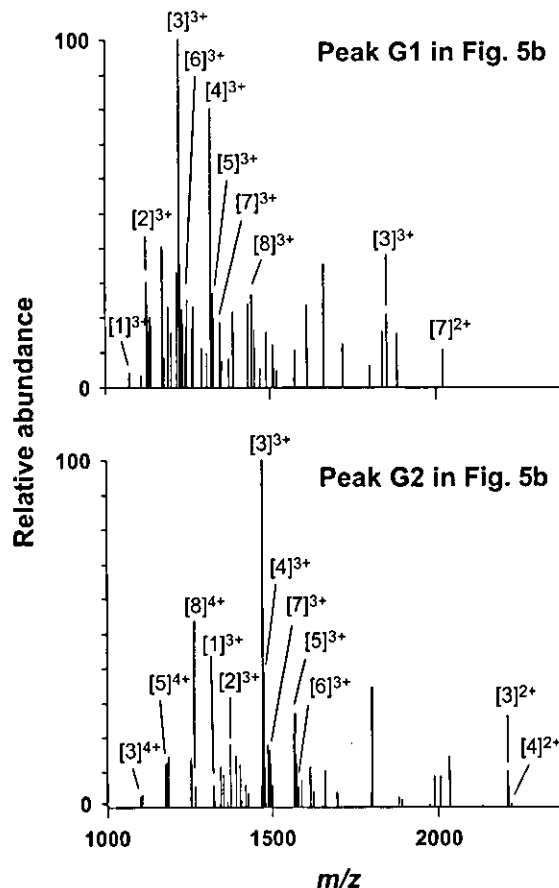


Fig. 6. Mass spectra of glycopeptides in peaks G1 and G2 in Fig. 5b. The observed m/z value of each ion is summarized in Table 4.

were assigned to glycosylated D5 and D15-1, respectively. The oligosaccharides attached to each *N*-glycosylation site were deduced as shown in Table 4. By comparing the *N*-linked oligosaccharide structures on

Asn95 with those on Asn259, it was concluded that biantennary oligosaccharides are major oligosaccharides located at both Asn95 and Asn259, whereas the triantennary structures are present mainly at Asn95.

Table 3
Assignment of the peaks in Fig. 5a

Peak no. ^a	Peptide ^b	Theoretical mass ^c	Observed m/z ^d					
			M^+	M^{2+}	M^{3+}	M^{4+}	M^{5+}	M^{6+}
1	D4	2666.0	—	1334.2	889.9	667.4	—	—
2	D14	777.8	778.6	—	—	—	—	—
3	D15-2 ^e	1018.0	1019.0	510.4	—	—	—	—
4	D11	1456.6	1457.5	729.0	486.3	—	—	—
5	D6	4378.8	—	—	1460.8	1095.5	—	—
6	D8	3326.4	—	1664.6	1109.5	—	—	—
	D10	1467.6	1468.2	734.8	490.1	—	—	—
7	D1	4728.1	—	—	1577.0	1183.2	947.0	789.6
8	D7	1329.4	1330.2	665.3	—	—	—	—
9	D5	1608.7	1609.3	805.1	—	—	—	—
10	D9	4165.6	—	—	1389.0	1042.2	834.1	—
11	D15-1 ^e	2350.6	—	1176.2	784.2	—	—	—
12	D3	3219.5	—	1610.1	1073.8	806.4	—	—

^a Peak label in Fig. 5a.

^b Predicted peptides were shown in Fig. 1.

^c Calculated average mass.

^d Mass of the ions measured in the positive-ion ESI mass spectrum from precursor-ion scan.

^e Peptide derived from D15 peptide.

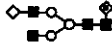
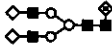
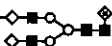
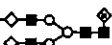
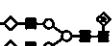
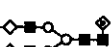
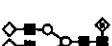
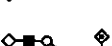

4. Discussion

The aim of the present study was to analyze the distribution of the glycoforms and the carbohydrate structures of rhFS. Previous study of FS isolated from porcine ovary has shown that porcine FS exists in six isoforms, due to alternative splicing and the site occupancy of N-linked oligosaccharides [8]. In this study, we used rhFS288 to eliminate the heterogeneity due to alternative splicing. The results of SDS-PAGE and MALDI-TOF MS revealed the presence of both non-glycosylated and glycosylated forms (Figs. 2 and 3). FS contains two potential *N*-glycosylation sites. Using mass spectrometric peptide/glycopeptide mapping and precursor-ion scanning, we found that both *N*-glycosylation sites were partially glycosylated (Fig. 5 and Table 3). Non-glycosylated and glycosylated proteins containing Asn95 and Asn259 were detected in the peptide/glycopeptide map and precursor-ion scanning, respectively. Monosaccharide composition analyses suggested the presence of linkages of fucosylated bi- and triantennary complex-type oligosaccharides on rhFS (Table 1). This finding was supported by mass spectrometric oligosaccharide profiling, in which the *m/z* values and

elution times of some of the oligosaccharides from rhFS were in good agreement with those of standard oligosaccharides. The site-specific glycosylations were deduced on the basis of the mass spectra of glycopeptides. It was suggested that biantennary oligosaccharides attach to both Asn95 and Asn259, whereas triantennary oligosaccharides attach mainly to Asn95 (Fig. 6 and Table 4).

Asn95 is located in the follistatin domain I, which is thought to be the heparin-binding site [26]. The site occupancy and structure of *N*-linked oligosaccharides on Asn95 may affect the heparin-binding ability of FS. Heparin/heparan sulfate proteoglycans are known to exert an important influence on FS, which neutralizes the activity of activins. It is therefore possible that sialylated oligosaccharides at Asn95 control the activin-neutralizing activity via modulation of the heparin-binding ability of FS. In fact, it was reported that the *N*-glycosylation isoforms of antithrombin and heparin cofactor II differ substantially in their affinity for heparin [27,28]. We are currently studying the role played by oligosaccharides in the activin-neutralizing activity of FS; these studies employ the carbohydrate remodeling technique using the CHO cell line established in the present study.

Table 4
Putative structures of *N*-linked oligosaccharides deduced from the LC/MS of the glycopeptides corresponding to the Asn95 and Asn259

Carbohydrate Structure ^a	Asn95					Asn259				
	Ions in peak G1	Theoretical mass ^b	Observed <i>m/z</i> ^c			Ions in peak G2	Theoretical mass ^b	Observed <i>m/z</i>		
			M ²⁺	M ³⁺	M ⁴⁺			M ²⁺	M ³⁺	M ⁴⁺
	1	3216.2	-	1073.4	-	1	3958.1	-	1319.6	-
	2	3378.6	-	1126.6	-	2	4120.5	-	1373.9	-
	3	3669.6	1835.7	1223.2	-	3	4411.5	2206.3	1471.8	1104.7
	-	-	-	-	-	4	4427.5	2214.8	1475.7	-
	4	3960.9	-	1320.6	-	5	4702.8	-	1569.5	1177.1
	5	3976.6	-	1326.8	-	6	4718.8	-	1574.5	-
	6	3743.7	-	1248.6	-	7	4485.6	-	1497.2	-
	7	4034.9	2017.5	1346.9	-	-	-	-	-	-
	8	4326.2	-	1444.1	-	8	5068.1	-	-	1267.6

^a Proposed structures based on molecular weight. Symbols: solid squares, GlcNAc; open circles, mannose; open diamonds, galactose; dotted diamonds, fucose; solid circle, NeuAc; dotted circle, NeuGc.

^b Calculated average mass.

^c Mass of the ion measured in the positive-ion ESI mass spectrum from precursor-ion scan. Mass spectra were shown in Fig. 6.